International Journal of Pharmaceutics 692 (2026) 126645

Contents lists available at ScienceDirect

International Journal of Pharmaceutics

journal homepage: www.elsevier.com/locate/ijpharm

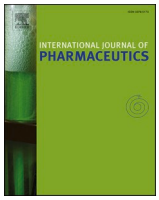

Engineering micro- and nanosized pharmaceutical salt crystals using high-pressure homogenization

Md Sadeque Hossein Mithu [a], Saumil Bhatt [a], Vivek Garg [d], Vivek Trivedi [c], Dennis Douroumis [a,b,*]

[a] Cubic Pharmaceuticals Ltd., Unit 3, Neptune Close, Medway City Estate, Rochester, Kent ME2 4LU, UK
[b] School of Life and Health Sciences, Department of Health Sciences, Pharmacy, University of Nicosia, No. 17, 29th Street, Elliniko, 167 77 Athens, Greece
[c] Medway School of Pharmacy, University of Kent, Medway Campus, Central Avenue, Chatham Maritime, Chatham, Kent ME4 4TB, UK
[d] Wolfson Centre for Bulk Solids Handling Technology, Faculty of Engineering & Science, University of Greenwich, Central Avenue, Chatham ME4 4TB, UK

ARTICLE INFO

Keywords:
Nanoparticles
Microparticles
High pressure homogenization
Salts
Surfactants

ABSTRACT

This study presents an innovative application of high-pressure homogenization (HPH) for the synthesis of micro- and nanocrystalline pharmaceutical salts, offering a scalable and environmentally sustainable alternative to conventional crystallization techniques. Using ketoconazole (KTZ) and oxalic acid (OA) as a model system, salt formation was successfully achieved through HPH processing in the presence of various stabilizers (Pharmacoat® 606, Pluronic® F127, Soluplus®, and TPGS) at different concentrations and process temperatures. Structural analysis by XRPD and FT-IR confirmed the formation of a new multicomponent salt through proton transfer and hydrogen bonding, while SEM imaging revealed controlled crystal morphology and significant particle size reduction to the submicron range. The process demonstrated remarkable reproducibility and flexibility, allowing morphological tuning through simple adjustments in stabilizer concentration and temperature. Dissolution studies performed at pH 4.4 showed up to an 80% drug release within 15 min for HPH-processed KTZ:OA salts, a substantial improvement over bulk KTZ. The findings establish HPH as a versatile, solvent-free, and continuous manufacturing platform for the production of high-purity pharmaceutical salts with superior dissolution performance, highlighting its potential to transform solid-state drug formulation and process intensification strategies in pharmaceutical development.

1. Introduction

Nanosizing drug particles is a widely recognized strategy to improve the dissolution rate and bioavailability of BCS class II drugs by increasing their surface area and saturation solubility (Shegokar and Müller, 2010). According to the Noyes–Whitney equation, enhanced solubility accelerates dissolution, while higher drug concentration in the gastrointestinal lumen increases the concentration gradient, promoting diffusion and absorption (Keck and Mu, 2006). Nanosized formulations also require lower excipient levels, achieving higher local drug concentrations while reducing potential excipient-related toxicity (Shegokar and Singh, 2011). Despite these advantages, only a limited number of nanocrystal-based pharmaceutical products have reached the market, although further product launches are anticipated (Malamatari et al., 2018). In the United States, nanocrystal technology is featured in 85 active patents with an additional 48 pending (Douroumis and Fahr, 2013).

Another approach to increase drug solubility and hence dissolution rates especially for the ionisable compounds. involves the formation of multicomponent products such as cocrystals and salt (Mithu et al., 2021; Malamatari et al., 2017). There is a number of processing technologies that have been successfully employed for the formation of multicomponent crystals, including solvent evaporation, slurry crystallization, mechanochemical processing, antisolvent preparation, extrusion, and supercritical fluid processing (Chadha et al., 2016; Serajuddin, 2007; Martin et al., 2013; Almeida e Sousa et al., 2016; Elder et al., 2013).

High-pressure homogenization (HPH) has emerged as an effective method to produce nanosized drug particles, adapted from food and biotechnology applications (Douroumis and Fahr, 2013; Mithu et al., 2021; Malamatari et al., 2017; Akanda et al., xxxx; McClements, 2011; Georget et al., 2014; Diels and Michiels, 2006; Fernández-Ronco et al., 2013). In this process, a fluid product is forced through a narrow nozzle

* Corresponding author at: School of Life and Health Sciences, Department of Health Sciences, Pharmacy, University of Nicosia, No. 17, 29th Street, Elliniko 167 77, Athens, Greece

https://doi.org/10.1016/j.ijpharm.2026.126645
Received 4 December 2025; Received in revised form 29 January 2026; Accepted 30 January 2026
Available online 3 February 2026

Table 1
Different formulations of KTZ and oxalic acid with various polymers and surfactants.

Exp. No	Stabilizers	Amount (w/v %)	Temp. (°C)	Drug/former: stabilizer ratio
1	Pharmacoat 606	0.25	25.0	4:1
2	Pharmacoat 606	0.50	25.0	3:1
3	Pluronic F127	0.25	25.0	4:1
4	Pluronic F127	0.50	25.0	3:1
5	Soluplus	0.25	25.0	4:1
6	Soluplus	0.50	25.0	3:1
7	TPGS	0.25	25.0	4:1
8	TPGS	0.50	25.0	3:1

Table 2
Different formulations of KTZ and OA with various polymers and surfactants at 40 °C.

Exp. No	Stabilizers	Amount (w/v%)	Temperature (°C)	Drug/ former: stabilizer ratio	Hansen solubility parameter (δ, $MPa^{1/2}$)
9	Pharmacoat 606	0.5	40	3:1	27.8
10	Pluronic F127	0.5	40	3:1	21.0
11	Soluplus	0.5	40	3:1	20.7
12	TPGS	0.5	40	3:1	23.8

δ_{KTZ}: 25.4 $MPa^{1/2}$.

under high pressure, reducing particle size and increasing surface area and free energy. However, particles below ~ 30 μm are prone to aggregation due to van der Waals and electrostatic forces, which can decrease effective surface area and negatively impact dissolution and bioavailability (Loh et al., 2014). Polymers are commonly employed as stabilizers during and after HPH to prevent agglomeration, while simultaneously enhancing solubility, wettability, and bioavailability. Stabilizer selection is typically empirical, with generally recognized as safe (GRAS) excipients widely used (Malamatari et al., 2018).

In this study, ketoconazole (KTZ) and oxalic acid (OA) were selected as a model API and salt former to produce nanosized salt crystals via HPH. Four polymers—Pharmacoat® 606 (HPMC), Pluronic® F127, Soluplus®, and TPGS—were evaluated as stabilizers. HPMC has been shown to produce nanocrystals as small as 70–120 nm for various APIs, with its hydrophobic segments facilitating surface adsorption and particle stabilization (Lee et al., 2008; Tuomela et al., 2016). Pluronic® F127, an amphiphilic block copolymer of polypropylene oxide and polyethylene oxide, has demonstrated superior stabilization compared to traditional homopolymers and has been used effectively in indomethacin and itraconazole nanosuspensions (Liu et al., 2015; Lu et al., 2014). TPGS has broad pharmaceutical applicability and has been successfully used to produce memantine–pamoic acid nanocrystals via HPH (Tuomela et al., 2016; Mittapelly et al., 2016). Soluplus®, a graft copolymer composed of polyethylene glycol, polyvinyl acetate, and polyvinyl caprolactam, has been employed in celecoxib nanoparticle formation using anti-solvent precipitation combined with HPH (Homayouni et al., 2014). The KTZ:OA salt (stoichiometric ratio 1:1.1) has previously been prepared via solvent evaporation and slurry crystallization, providing a suitable model system for nanosizing studies (Martin et al., 2013; Hiendrawan et al., 2015).

Overall, HPH combined with appropriate polymer stabilizers offers a versatile and scalable approach to produce stable nanosized pharmaceutical salts, enhancing dissolution, solubility, and ultimately bioavailability.

2. Materials and methods

2.1. Materials

Ketoconazole (KTZ), oxalic acid (OA), Pluronic® F-127, and D-α-tocopheryl polyethylene glycol 1000 succinate (TPGS) were purchased by Sigma-Aldric, UK. Soluplus® (Polyvinyl caprolactame- polyvinyl acetate-polyethylene glycol graft) was kindly donated by BASF (Germany). Reagents of HPLC grade such as methanol and acetonitrile were purchased from Fisher Chemicals (Loughborough, UK). The solids and solvents were used as received without further purification.

2.2. High-pressure homogenisation

High pressure homogenization was employed for the processing of the drug and salt former solutions for the synthesis of the salts. Specifically, physical mixtures (1 g) of KTZ and OA (stoichiometric ratio 1:1.1) were dissolved in a solvent mixture (2% w/v) of acetone and methanol (1:1) and then homogenised in 50 mL of the aqueous phase (with or without the stabilizers). The role of various polymers as stabilisers was investigated; for this purpose, 0.25% and 0.50% (w/v) of polymers were added to the aqueous phase and stirred for 30 min until were fully dissolved (Table 1). After the addition of polymer, the resulting clear solution was rapidly transferred and homogenised in a MicroDebee laboratory homogeniser (South Easton, MA, USA) at 15,000 psi for a predetermined time at room temperature. The homogenization process was repeated for selected formulations this time by applying temperatures of 40 °C for the same period (Table 2). At the end of the homogenisation process, the samples were subjected to vacuum filtration using a borosilate Buchner kit (Millipore XX1004700) with PTFE (polytetrafluoroethylene) filters (0.1 μm) to remove the aqueous/organic solutions. The process was applied for another 10 min to dry the cocrystals. The filtrate was dried overnight at 50 °C and stored for further analysis.

2.3. Differential scanning calorimetry (DSC)

Bulk compounds, physical mixture (PM) of API and coformer and collected solid products from three different processing by HPH were analysed using a DSC (Mettler Toledo 823e, Greifensee, Switzerland). All the samples were accurately weighed (2 to 4 mg) and placed into aluminium pans and transferred to the sample holder. Samples were then heated over the required temperature range (depending on their melting point), starting from 0 °C or 25 °C up to 300 °C at a scan rate of 10 °C/min under an atmosphere of nitrogen gas using a flow of 50 mL/min. STARe software was used to analyse the data obtained from the samples.

2.4. Powder X-ray diffraction (PXRD)

PXRD data of all the bulk samples, PM and final products prepared by HPH processing were collected using a D8 Advanced X-ray diffractometer (Bruker, Germany). A Cu anode powered at 40 kV and 40 mA, a primary 4° Soller slit and a secondary 2.5° Soller slit, and a 0.2 mm exit slit was selected for all experiments. The samples were rotated at 15 RPM (rotation per minute) with a step size set at 0.02°2θ and the counting time set at 0.2 sec per step. Few milligrams of dried solids were placed on a sample holder and diffractograms were collected at a range of 2–55°2θ scale. A primary Göbel mirror was used for the parallel beam and the removal of Cu Kβ. EVA phase analysis (Bruker, Germany) software was used to analyse the data and compare the peak positions.

2.5. Cambridge structural database (CSD) search

All searches were carried out in the Cambridge structural database (CSD, Cambridge Crystallographic Data Centre). The search for ketoconazole cocrystals and salt was done by typing ketoconazole in

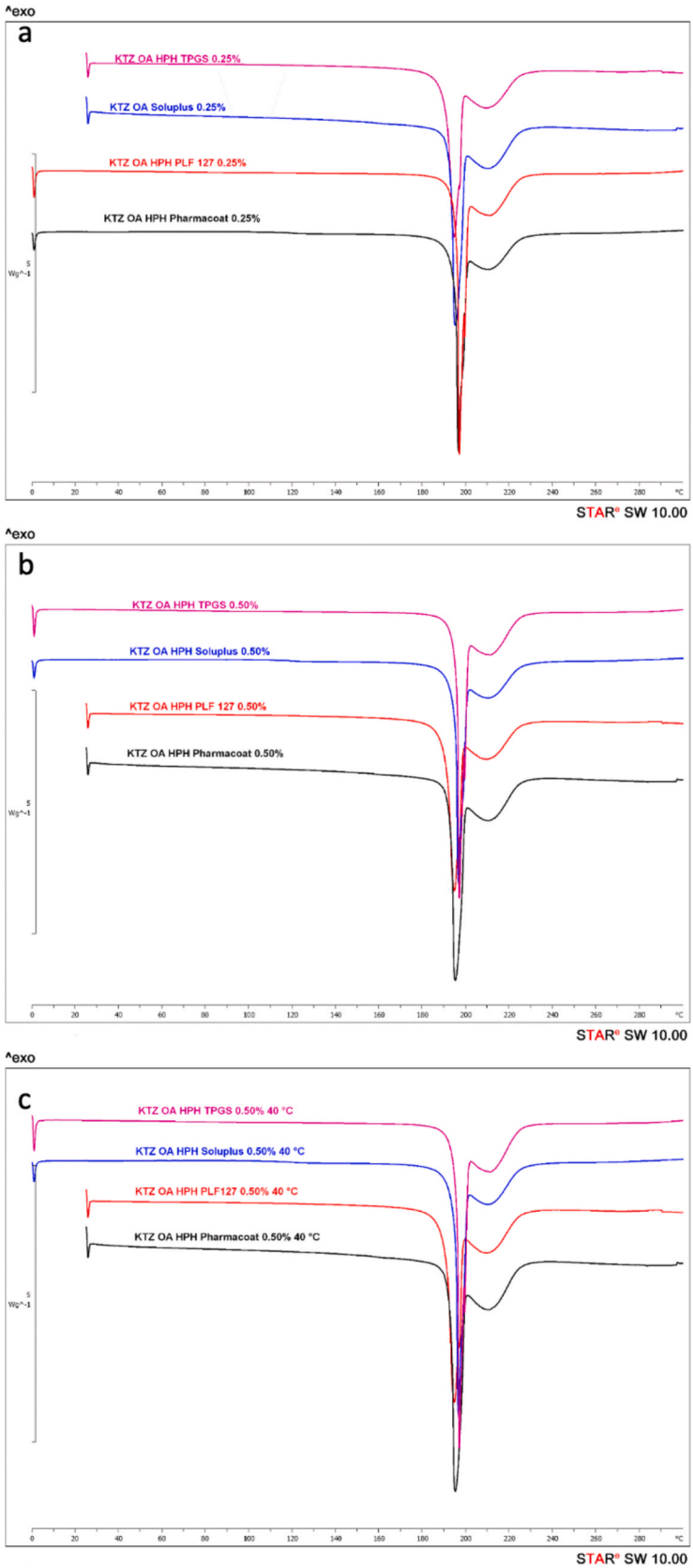

Fig. 1. DSC thermograms of KTZ-OA homogenised at a) 0.25% (w/v) concentrations of Pharmacoat®, Pluronic® 127, Soluplus® and TPGS at 25 °C, a) 0.50% (w/v) concentrations of Pharmacoat®, Pluronic® 127, Soluplus® and TPGS at 25 °C and c) 0.50% (w/v) concentrations of Pharmacoat®, Pluronic® 127, Soluplus® and TPGS at 40 °C.

compound name option in the access structure site. There were only two hits, which were not cocrystal/salt. Based on the published work of Martin et al. (2013) yielded four CIF files: ketoconazole cocrystals with fumaric (YINWAV), succinic (YINWEZ), and adipic (YINWID) acids, and ketoconazole oxalate salt (YINVUO). These were used in PXRD analysis with TOPAS to assess cocrystal and salt formation.

2.6. FTIR spectroscopy analysis

ATR-FTIR spectroscopy was performed for both the API and conformer, as well as for the solids obtained from the process using HPH, with a PerkinElmer Spectrum Two (UK) equipped with a ZnSe crystal. The ATR crystal, pressure plate, and tip were thoroughly cleaned before each background and sample scan to avoid cross-contamination. A small amount of sample was placed directly onto the crystal, and contact was ensured by adjusting the applied force using the metal tip. Spectra were collected over the range of 400–4000 cm^{-1} at a resolution of 4 cm^{-1}, with four scans averaged per spectrum.

2.7. Scanning electron microscopy (SEM)

The morphology of ketoconazole, oxalic acid, and the HPH processed products was examined using a SEM (Hitachi SU8030, Japan), operated at an accelerating voltage of 1 kV in backscattering mode. A small amount of each sample was mounted onto an aluminium stub using conductive adhesive and coated with a thin layer of chromium for approximately 3 min to enhance surface conductivity. Micrographs were acquired at various magnifications to evaluate and compare the morphological features of the samples.

2.8. In-vitro dissolution studies

Dissolution studies were conducted using a USP paddle apparatus method by employing a Varian 705 DS dissolution paddle apparatus (Varian Inc., North Carolina, US). Acetate buffer, pH 4.4 (glacial acetic acid and anhydrous sodium trihydrate) was used as dissolution media, the temperature was maintained at 37.5 ± 1 °C and the rotation speed of the shaft was set to 100 RPM. 100 mg of bulk KTZ and the equivalent amount of jet dispensed powder was placed into the apparatus containing 900 mL buffer. 5 mL of the sample was withdrawn from the apparatus after 15 min and it was replaced by 5 mL of buffer immediately. This process was repeated at different time intervals: 15, 30, 60, 90 and 120 min. The collected samples were then filtered and analysed by Agilent Technology 1200 series HPLC (Agilent Technologies, Cheadle, UK) using a Hichrom S50DS2 − 4889, (4.6 mm x 150 mm) column and a freshly prepared mobile phase consisting of methanol: water: triethylamine (80:20:0.02% v/v). The analysis was performed at a mobile phase flow rate of 1 mL/min on 20 µl sample at 240 nm. Collected data was analysed and integrated using Chemstation®.

2.9. Statistical analysis

Statistical analysis was performed for in-vitro dissolution performances of the synthesized salts using the Two-way ANOVA, and statistical significance was set at $p < 0.05$ using Fusion One software (DoE Fusion One TM, California, United States).

3. Results and discussion

3.1. HPH for nanocrystal salt synthesis

The formulation of poorly water-soluble active pharmaceutical ingredients (APIs) remains a major challenge in modern drug development. Among various nanonization technologies, nanocrystal production has emerged as an effective strategy to enhance dissolution rate, saturation solubility, and oral bioavailability. High-Pressure Homogenization operates via intense shear and cavitation forces under pressures up to 2000 bar, reducing coarse drug suspensions to nanoscale dimensions. It is a solvent-free, scalable, and industry-preferred top-down process that produces highly stable nanosuspensions with narrow particle size distribution (typically 100–500 nm). Its reproducibility and compatibility with aqueous stabilizers make it particularly suited for continuous manufacturing and regulatory compliance.

There are also other bottom-up precipitation approaches enable fine control over nucleation and crystal growth, producing particles as small as 50–400 nm. However, solvent–antisolvent systems complicate scale-up and solvent removal. Sonocrystallization for example combines acoustic cavitation and supersaturation control, providing a versatile laboratory-scale method for screening polymorphs and co-crystals, though limited by batch processing and energy efficiency.

Among those technologies, HPH is a preferred approach due to its robust scalability, environmental friendliness, and ability to integrate salt formation and particle size reduction within a single process step. It has demonstrated success in generating nanocrystals of drugs such as ketoconazole, fenofibrate, and itraconazole, leading to significantly improved dissolution and bioavailability (Anna Karagianni et al., 2020; Ige et al., 2013; Vadher et al., 2024). Overall, while all four methods offer distinct benefits, HPH remains the most versatile and industrially adaptable nanocrystal production platform for poorly soluble pharmaceuticals. Hence we introduce for first time the use of HPH for the synthesis of salt nanocrystals by using KTZ:OA as model drug-former pair. The key processing parameters were the applied pressure and temperature of the homogenizer that were considered (Potta et al., xxxx) for the salt synthesis and particle engineering. In addition, the aqueous/organic phase ratio was another critical material attribute which was kept at 25:1 based on previous work (Schlindwein and Gibson,).

3.2. Solid state analysis

DSC analysis was performed to investigate the thermal events occurred in the bulk solid and freshly made cocrystals made by HPH process. Fig. 1a, illustrates the obtained thermograms where KTZ presented a sharp endothermic melting point at 150 °C while for OA it was detected at 192 °C respectively. The synthesized cocrystal of KTZ OA (1:1.1) produced through the HPH process revealed a unique single endothermic peak at 197 °C.

From Fig. S1 it is obvious that no other endothermic event was noticed the melting peak of the HPH processed materials was different to those of the parent materials, suggesting the formation of a new crystalline structure. The comparison with the previously reported KTZ:OA salt data from Martin *et al.* (2013), KTZ OA (1:1.1) showed a very similar melting point with an endothermic peak at 198 °C which confirmed the formation of KTZ oxalate salt via HPH (Martin et al., 2013). Similarly, DSC analysis was carried out for the samples where stabilisers (Pharmacoat, Pluronic, Soluplus and TPGS were dissolved in the aqueous phase which was used for the HPH process. Notably, the thermal behaviour of the newly formed crystals was similar to initially HPH processed KTZ:OA, in the absence of any stabiliser. As shown in Fig. 1 all stabilisers resulted in the formation of oxolate salt with sharp endothermic peaks at 197 °C. As shown in Table 2 the stabilizers presented similar solubility parameter (δ) to bulk KTZ and hence the Δδ was <7 (Li and Chiappetta, 2008; Jiannan et al., 2016; Jankovica et al., 2019; Kitak et al., 2015). However, the DSC analysis showed that the stabilisers have no effect on the KTZ solubilisation for concentrations varying from 0.25 to 0.50% and eventually in the purity of the synthesised cocrystals. As previously mentioned HPH processing was also performed at 40 °C to investigate the effect of stabilisers at elevated temperatures. Similarly, the utilization of higher processing temperatures in combination with the applied pressure during the HPH process did not affect the formation of the oxolate salts where sharp melting endotherms appeared at the same temperature.

Furthermore, the bulk materials and products obtained by HPH were

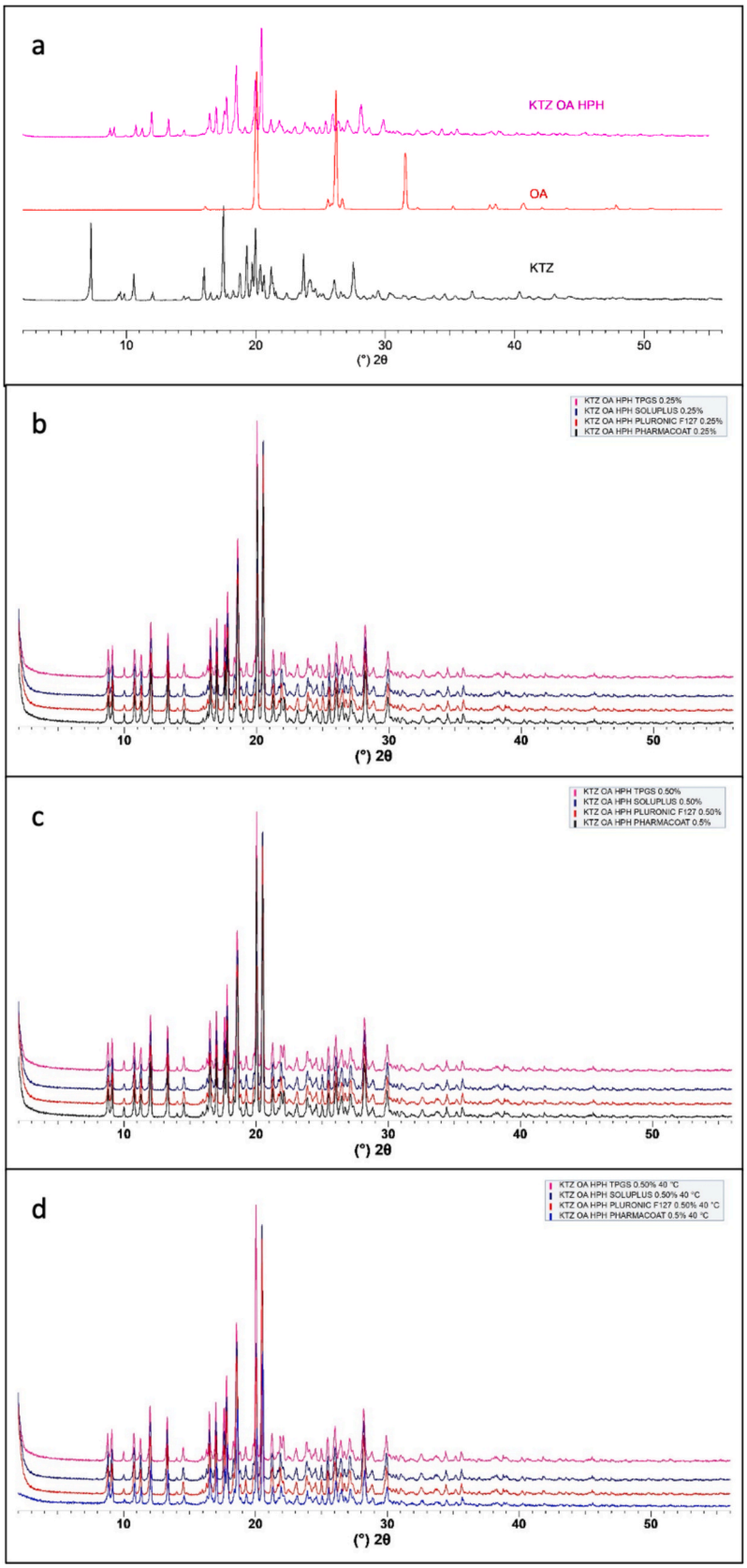

Fig. 2. Diffraction patterns of a) bulk KTZ, OA, and KTZ-OA salt, b) KTZ-OA salts processed with HPH in the presence of 0.25% stabilizers at 25 °C, c) KTZ-OA salts processed with HPH in the presence of 0.50% stabilizers at 25 °C, and d) KTZ-OA salts processed with HPH in the presence of 0.5% stabilizers at 40 °C.

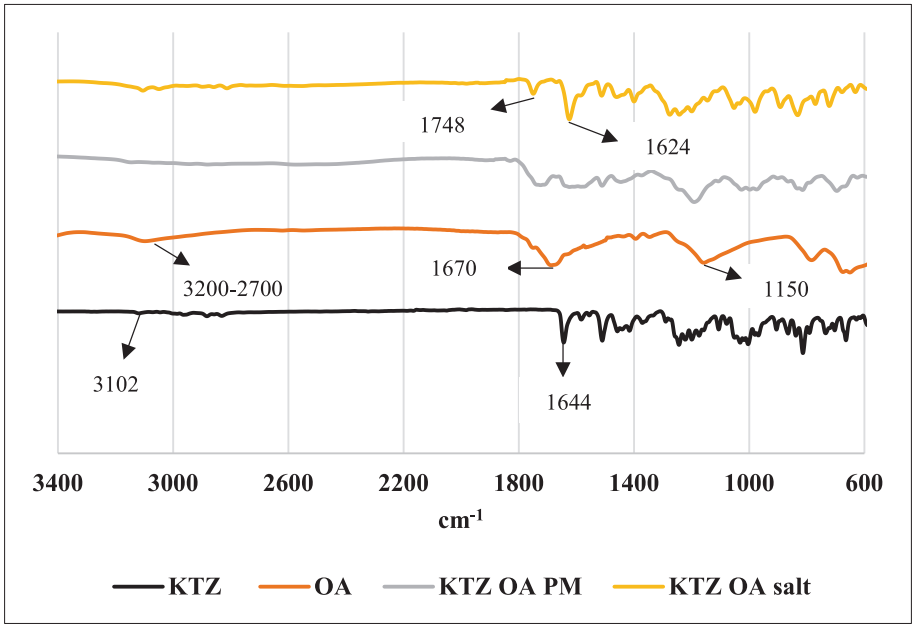

Fig. 3. FTIR spectroscopic analysis of bulk materials and KTZ-OA salt produced by HPH.

also analysed by PXRD to identify variations in the diffraction patterns. The obtained data were compared with previously reported results from the Cambridge Structural Database (CSD) using TOPAS software. The degree of correspondence between the newly acquired crystal data and the CSD reference data was evaluated through Rietveld refinement performed with TOPAS V4.2. Although visual agreement of the crystalline peaks is important for assessing the quality of fit, it is generally accepted that a refinement is satisfactory when the weighted profile R factor (Rwp) is within approximately three times the expected R factor (Rexp) (Toby, 2006). The principal diffraction peaks for KTZ were observed at 2θ values of 7.28°, 9.50°, 10.69°, 11.96°, 16.13°, 17.50°, 20.01°, and 27.65° (Table 2). The salt former, OA, exhibited diffraction peaks at 16.09°, 19.03°, 20.11°, 26.24°, and 31.57° 2θ.

As presented in Fig. 2a, distinct and well-defined crystalline profiles were obtained for the KTZ:OA salts following HPH processing. For the synthesized salt characteristic peaks observed at 2θ values of 8.75°, 10.81°, 11.95°, 13.27°, 17.72°, 18.50°, 19.89°, 20.42°, and 28.14°. The diffraction peaks recorded for the formed oxalate differed significantly from those of the bulk KTZ and OA crystals, confirming the formation of a new crystalline phase. Furthermore, comparison of the obtained KTZ:OA diffractograms with the reference data reported in the Cambridge Structural Database (CSD) by Martin *et al.* (Martin et al., 2013) revealed close agreement in peak positioning. This correspondence was further verified through Rietveld refinement, where the weighted profile R factor (Rwp) was found to be within twice the expected R factor (Rexp) (Fig. S2, supplementary), indicating an excellent fit between the experimental and simulated data. Similarly, X-ray powder diffraction (XRPD) analysis was carried out on the HPH-processed samples prepared in the presence of stabilizers at concentrations of 0.25% and 0.5% (Fig. 2b, c). The obtained diffractograms displayed identical diffraction patterns, with consistent peak intensities and positions at the same 2θ values, irrespective of the stabilizer concentration used. Moreover, as shown in Fig. 2d, the samples processed with 0.5% stabilizer at elevated HPH temperatures (40 °C) exhibited diffraction profiles comparable to those obtained under standard conditions. These findings indicate that neither the concentration of stabilizers nor moderate increases in processing temperature significantly influenced the crystalline structure or phase purity of the HPH-derived salts, suggesting high process reproducibility and structural stability of the resulting solid forms. Overall, the XRPD analysis confirmed the successful formation of KTZ:OA salts via HPH, with the resulting crystalline solids exhibiting high phase purity and structural uniformity approaching 100%.

3.3. FTIR spectroscopy analysis

Fourier-transform infrared (FT-IR) spectra of bulk ketoconazole (KTZ), oxalic acid (OA), their physical mixture (PM), and the KTZ:OA salt obtained via HPH processing were collected to investigate possible molecular interactions between KTZ and OA. Comparison of the spectra between bulk materials and the synthesized salt was performed to confirm proton transfer between the salt former and the drug. As shown in Fig. 3, KTZ exhibited a characteristic broad N–H stretching vibration at 3125 cm^{-1}, while absorption bands at 1644 and 1370 cm^{-1} corresponded to carbonyl (C═O) stretching and C═C stretching of the aromatic ring, respectively (Tiago et al., 2013; Bezerra et al., 2025; Elder et al., 2007; Patel et al., 2011; Kamble et al., 2017; Shayanfar and Jouyban, 2014).

OA, containing two carboxylic acid (–COOH) groups, showed typical vibrational modes including O–H stretching, C═O stretching, C–O stretching, and both in-plane and out-of-plane O–H deformation vibrations. The O–H stretching band appeared in the 3200–2700 cm^{-1} region, with a prominent peak at 1670 cm^{-1} attributed to C═O stretching, and the C–O stretching vibration identified at 1150 cm^{-1} (Muthuselvi et al., 2016; Alatas et al., 2015).

In the FT-IR spectrum of the HPH synthesised KTZ:OA salt the C═O stretching band of KTZ shifted to 1624 cm^{-1}, accompanied by the emergence of a new peak at 1748 cm^{-1}. These shifts in vibrational frequencies for both KTZ and OA are indicative of supramolecular heterosynthon formation within the multicomponent salt. Additionally, the disappearance of the broad O–H stretching band of OA suggests the formation of hydrogen bonds in the KTZ:OA salt (Elder et al., 2007; Patel et al., 2011; Kamble et al., 2017). Similar results were obtained for the salts synthesized in the presence of stabilizers (data not shown).

3.4. Morphology and particle size studies

Nanocrystals were characterized using a combination of imaging and non-imaging techniques, with SEM selected for crystal size and morphology analysis due to precipitation issues observed during light scattering measurements (Peltonen et al., 2015; Cerdeira et al., 2013;

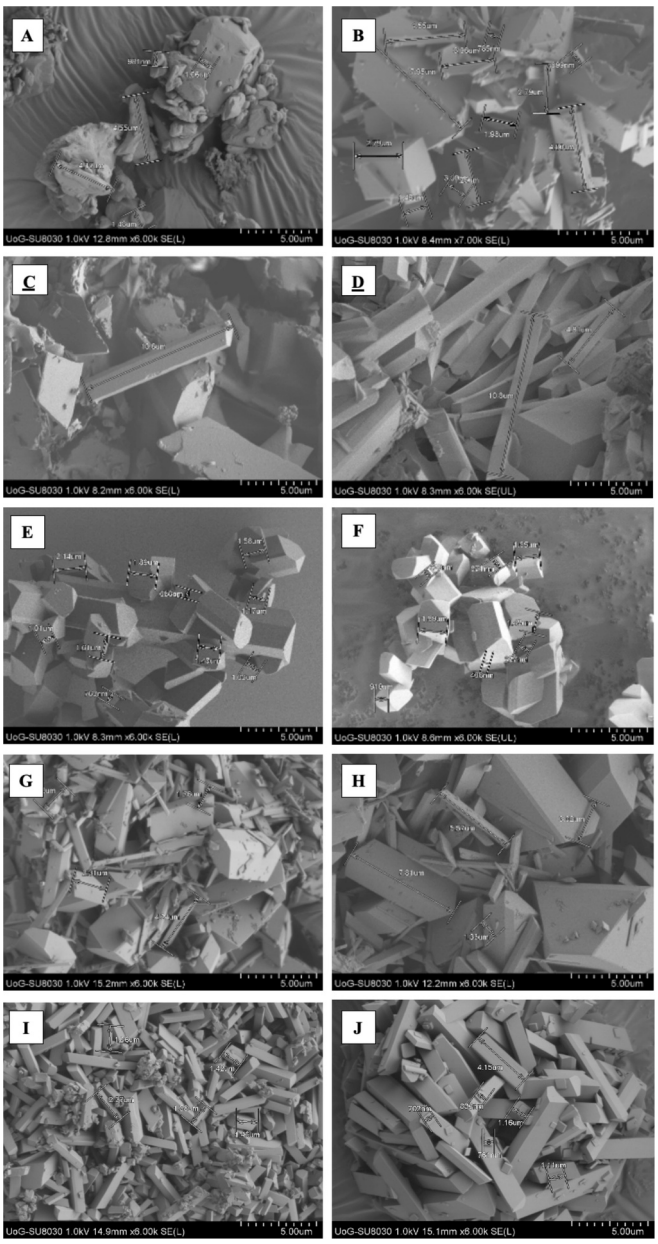

Fig. 4. SEM images of bulk KTZ (A) and KTZ/OA HPH crystals without stabiliser (B), KTZ OA – Pharmacoat® 606; 0.25% (C) and 0.5% (D); KTZ OA- Pluronic® F127; 0.25% (E) and 0.5% (F); KTZ OA- Soluplus®; 0.25% (G) and 0.5% (H); KTZ OA- TPGS; 0.25% (I) and 0.50% (J).

Peltonen, 2018). Bulk KTZ and HPH-synthesized KTZ-OA salts were compared, revealing that the salts formed irregular block- or rod-shaped crystals, with sizes ranging from 1 to 8 μm. A clear crystal lattice was observed in the KTZ-OA salts, absent in bulk KTZ (Fig. 4b).

The effects of stabilizers on crystal morphology and size were evaluated using Pharmacoat® 606, Pluronic® F127, Soluplus®, and TPGS. Pharmacoat® 606 (Fig. 4, C, D) produced thin, elongated rod-shaped crystals (nm to 4–10 μm), while Pluronic® F127 (Fig. 4, E, F) yielded prismatic, elongated crystals with parallel flat faces, with particle sizes reduced to 0.3–2 μm. Increasing Pluronic® F127 concentration (Schwarz and Mehnert, 1999) decreased crystal size further (Fig. 4, E, F). Soluplus® resulted in irregular morphologies combining thin rods and larger blocks (2–8 μm), showing minimal effect from concentration (Fig. 4, G, H)). TPGS stabilized slightly smaller prismatic crystals with elongated shapes, ranging from nm to 1–4 μm (Fig. 4, I, J). Overall, higher stabilizer concentrations produced smaller, more uniform crystals, consistent with prior reports emphasizing the need for optimized stabilizer levels to prevent aggregation or Ostwald ripening (Ito et al., 2016). A 0.5% (w/v) stabilizer concentration was therefore selected for further studies.

The impact of increasing HPH temperature from 25 °C to 40 °C was also examined. Pharmacoat® 606 (Fig. 5A) produced longer rod-shaped crystals with minimal deformation, while Soluplus® (Fig. 5B) and TPGS (Fig. 5C) yielded smaller, block-shaped crystals in the nano- to micrometer range. Pluronic® F127 generated predominantly 0.3–0.6 μm short prismatic crystals with minimal deformation (Fig. 5D).

During HPH, crystal agglomeration depends on activation energy, which stabilizers increase through steric and electrostatic mechanisms. Long-chain polymers create a physical barrier, whereas charged polymers reduce surface charge, both limiting aggregation (Van Eerdenbrugh et al., 2008; Verwey, 1947). Particle size reduction was consistent across homogenization cycles and applied pressure (Müller and Junghanns, 2008). Unlike previous reports of Pluronic® F127 destabilization at higher temperatures (Deng et al., 2010), the high-pressure environment likely inhibited micelle formation. The stabilizers were introduced at the beginning of the process, further supporting effective crystal size stabilization.

3.5. *In-vitro dissolution studies*

The dissolution behaviour of KTZ:OA salts homogenized with four different stabilizers at 40 °C was evaluated against bulk KTZ over a 120 min period to assess the impact of nanosizing and salt formation on dissolution performance. KTZ is known to exhibit pH-dependent solubility as weak base, dissolving readily in acidic environments (1–3) but demonstrating limited solubility under neutral and alkaline conditions (Adachi et al., 2015; Chen and Rodríguez-Hornedo, 2018). The dissolution rates in the pH range of 1–3, where no significant differences were observed between the parent compound and its salt forms. Therefore, dissolution studies were conducted at pH 4.4 to better differentiate the performance of the synthesized KTZ salts. Similar trends, with slightly lower dissolution rates, were also observed at pH 6.8 (unpublished data).

As shown in Fig. 6, all KTZ:OA salts co-processed with 0.5% (w/v) stabilizers exhibited a markedly faster dissolution rate compared with the parent compound. Bulk KTZ showed sluggish dissolution, reaching only 47% after 30 min and not exceeding 72% after 120 min. In contrast, the KTZ:OA salts displayed rapid dissolution within the first 15 min, achieving between 72% and 80% release.

The enhanced dissolution performance of the KTZ:OA salts can be attributed to a combination of factors, including reduced particle size, increased surface area, and improved wettability resulting from stabilizer adsorption during the high-pressure homogenization process. Moreover, the formation of the KTZ:OA salt likely modified the crystal lattice energy, contributing to improved solubility relative to the bulk drug. Interestingly, the nature of the stabilizer had minimal influence on the dissolution kinetics, suggesting that once a critical stabilizer concentration was reached, further improvements were dominated by intrinsic properties of the salt form rather than interfacial effects. Similar dissolution profiles were obtained for the KTZ:OA salts prepared with 0.25% (w/v) stabilizers (data not shown), indicating that both concentrations provided sufficient stabilization and surface modification to achieve enhanced drug release.

The KTZ–OA salt samples were stored under long-term stability conditions (25 °C/65% RH) and analysed by XRPD after 6 and 12 months; the results are summarised in Table 3. Rietveld refinement indicated that the crystalline purity remained unchanged at both time points and was comparable to that of the as-prepared sample. The 12-month stability evaluation demonstrated no significant alteration in the crystal behaviour of the salts produced via HPH processing when stored at 25 °C/65% RH. Nevertheless, a comprehensive stability study conducted under appropriate ICH-recommended conditions is required

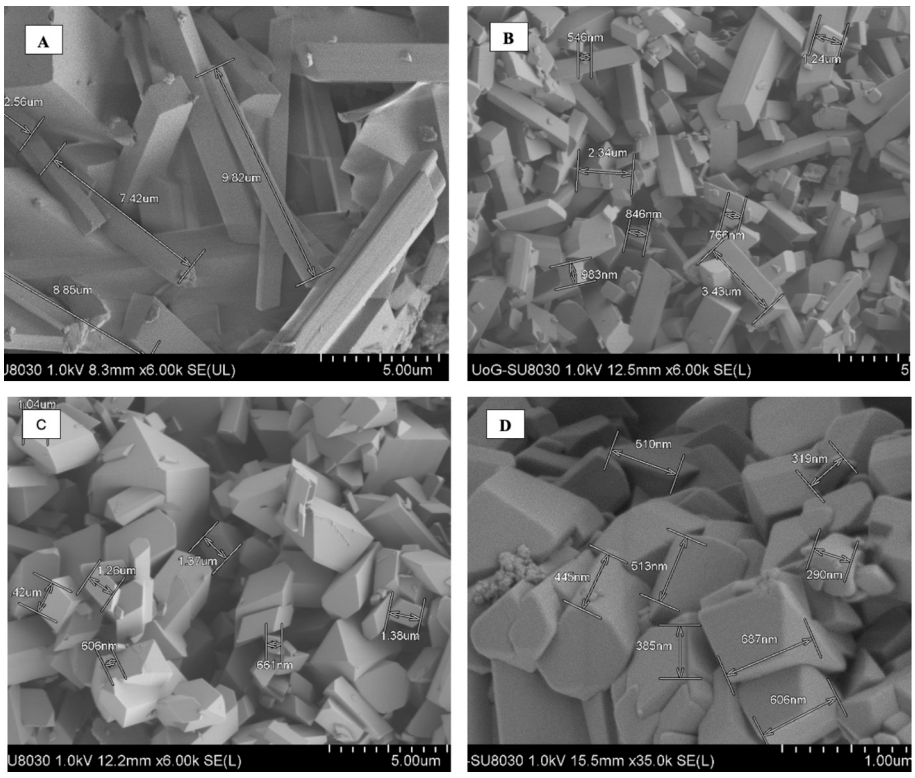

Fig. 5. SEM images of KTZ OA salt produced by HPH process with Pharmacoat® (A), Soluplus® (B), TPGS (C) and Pluronic® F127 (D) at 40 °C.

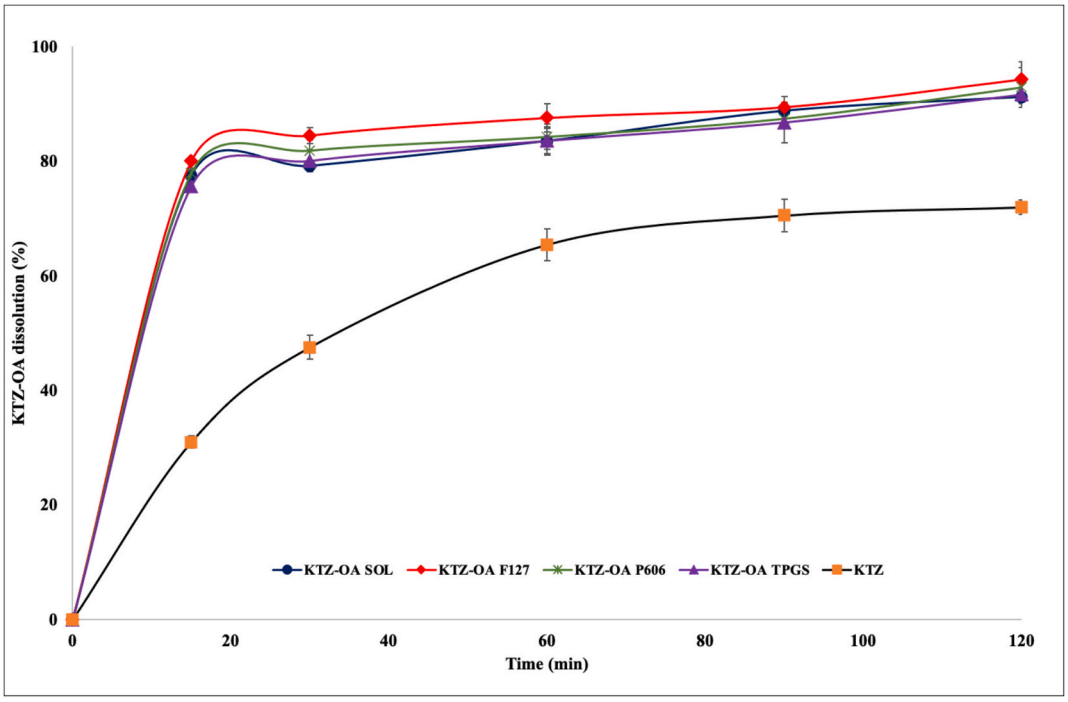

Fig. 6. Release profile of bulk KTZ and KTZ:OA salts co-processed with Pharmacoat®, Soluplus®, TPGS and Pluronic® F127 using HPH (the bars represent the STDV for the three different dissolution runs that was carried out for each sample).

to further confirm these findings.

4. Conclusions

The work demonstrates, for the first time, the feasibility of high-pressure homogenization as a direct synthesis route for pharmaceutical salts in the micro- to nanoscale range. This process integrates particle size reduction, salt formation, and stabilization in a single, solvent-free step, representing a significant advancement over traditional solid-state and solution-based crystallization methods. The ability to modulate crystal morphology and purity through simple control of processing parameters and stabilizer selection underscores the

Table 3
Comparison of KTZ:OA salt purity for as-made, and under 6 and 12-months storage stability.

Sample	Cocrystal purity (%)	
	6 M 25 °C/65% RH	12 M 25 °C/65% RH
KTZ: OA	99.9	99.9
KTZ: OA:Pharmacoat®	99.9	99.9
KTZ: OA:Soluplus®	99.9	99.9
KTZ: OA: Pluronic®	99.9	99.9
KTZ: OA:TPGS	99.9	99.9

technique's formulation adaptability and scalability. The superior dissolution performance of the KTZ:OA salts further confirms the potential of HPH-derived materials to enhance the bioavailability of poorly soluble drugs. Collectively, these results position HPH as a next-generation platform for nanocrystal and salt engineering, enabling greener and more efficient pharmaceutical manufacturing.

CRediT authorship contribution statement

Md Sadeque Hossein Mithu: Writing – original draft, Validation, Methodology, Investigation, Formal analysis, Data curation. **Saumil Bhatt:** Validation, Supervision, Software, Resources, Project administration, Funding acquisition. **Vivek Garg:** Writing – review & editing, Supervision, Software, Resources, Methodology, Investigation, Data curation. **Vivek Trivedi:** Writing – review & editing, Supervision, Software, Resources, Investigation, Formal analysis, Data curation. **Dennis Douroumis:** Writing – review & editing, Writing – original draft, Visualization, Validation, Supervision, Resources, Project administration, Methodology, Funding acquisition, Formal analysis, Conceptualization.

Declaration of competing interest

The authors declare that they have no known competing financial interests or personal relationships that could have appeared to influence the work reported in this paper.

Acknowledgements

This project has received funding from the Interreg 2 Seas programme 2014-2020 co-funded by the European Regional Development Fund under subsidy contract 2S01-059_IMODE.

Appendix A. Supplementary data

Supplementary data to this article can be found online at https://doi.org/10.1016/j.ijpharm.2026.126645.

Data availability

Data will be made available on request.

References

Adachi, M., Hinatsu, Y., Kusamori, K., et al., 2015. Improved dissolution and absorption of ketoconazole in the presence of organic acids as pH-modifiers. Eur. J. Pharm. Sci. 76, 225–230.
M Akanda, MDSH Mithu, D Douroumis. Solid lipid nanoparticles: An effective lipid-based technology for cancer treatment. Drug Deliv. Sci. Techn., 104709.
Alatas, F., Ratih, H., Soewandhi, S.N., 2015. Enhancement of solubility and dissolution rate of telmisartan by telmisartan-oxalic acid co-crystal formation. Int J Pharm Pharm Sci 7 (3), 423–426.
Almeida e Sousa, L., Reutzel-Edens, S.M., Stephenson, G.A., Taylor, L.S., 2016. Supersaturation potential of salt, co-crystal, and amorphous forms of a model weak base. Cryst. Growth Des. 16 (2), 737–748.
Bezerra, R.D.S., Domingos, F.N.B., dos Santos, A.O., da Silva, L.M., Ayala, A.P., Souto, E. B., da Silva, L.F.L., de Sousa, F.F., Lang, R., de Oliveira Neto, J.G., 2025. A novel ethionamide–phthalic acid salt with improved dissolution for tuberculosis therapy: insights from structural, spectroscopic, and DFT-periodic calculations analyses. Cryst. Growth Des. 25 (15), 6345–6361.
Cerdeira, A.M., Mazzotti, M., Gander, B., 2013. Formulation and drying of miconazole and itraconazole nanosuspensions. Int. J. Pharm. 443, 209–220.
Chadha, R., Singh, P., Khullar, S., Mandal, S.K., 2016. Ciprofloxacin hippurate salt: crystallization tactics, structural aspects, and biopharmaceutical performance. Cryst. Growth Des. 16 (9), 4960–4967.
Chen, Y.M., Rodríguez-Hornedo, N., 2018. Cocrystals mitigate negative effects of High pH on solubility and dissolution of a basic drug. Cryst. Growth Des. 18 (3), 1358–1366.
Deng, J., Huang, L., Liu, F., 2010. Understanding the structure and stability of paclitaxel nanocrystals. Int. J. Pharm. 390 (2), 242–249.
Diels, A.M.J., Michiels, C.W., 2006. High-pressure homogenization as a non-thermal technique for the inactivation of microorganisms. Crit. Rev. Microbiol. 32 (4), 201–216.
Douroumis, D., Fahr, A., 2013. Drug Delivery Strategies for Poorly Water-Soluble Drugs. Wiley & Sons.
Elder, E.J., Evans, J.C., Scherzer, B.D., Hitt, J.E., Kupperblatt, G.B., Saghir, S.A., Markham, D.A., 2007. Preparation, characterization, and scale-up of ketoconazole with enhanced dissolution and bioavailability. Drug Dev. Ind. Pharm. 33 (7), 755–765.
Elder, D.P., Holm, R., De Diego, H.L., 2013. Use of pharmaceutical salts and cocrystals to address the issue of poor solubility. Int. J. Pharm. 453 (1), 88–100.
Fernández-Ronco, M.P., Kluge, J., Mazzotti, M., 2013. High pressure homogenization as a novel approach for the preparation of co-crystals. Cryst. Growth Des. 13 (5), 2013–2024.
Georget, E., Miller, B., Callanan, M., Heinz, V., Mathys, A., 2014. (Ultra) high pressure homogenization for continuous high pressure sterilization of pumpable foods- a review. Front. Nutr. 1, 1–6.
Hiendrawan, S., Hartanti, A.W., Veriansyah, B., Widjojokusumo, E., Tjandrawinata, R.R., 2015. Solubility enhancement of ketoconazole via salt and cocrystal formation. Int. J. Pharm. Pharm. Sci. 7 (7), 160–164.
Homayouni, A., Sadeghi, F., Varshosaz, J., Afrasiabi Garekani, H., Nokhodchi, A., 2014. Promising dissolution enhancement effect of soluplus on crystallized celecoxib obtained through antisolvent precipitation and high pressure homogenization techniques. Colloids Surf. B Biointerf. 122, 591–600.
Ige, P.P., Baria, R.K., Gattani, S.G., 2013. Fabrication of fenofibrate nanocrystals by probe sonication method for enhancement of dissolution rate and oral bioavailability. Colloids Surf. B Biointerf. 108, 366–373.
Ito, A., Konnerth, C., Schmidt, J., Peukert, W., 2016. Effect of polymer species and concentration on the production of mefenamic acid nanoparticles by media milling. Eur. J. Pharm. Biopharm. 98, 98–107.
Jankovica, Sandra, Tsakiridou, Georgia, Ditzingera, Felix, Koehle, Niklas J., Pricef, Daniel J., Iliee, Alexandra-Roxana, Kalantzi, Lida, Kimpe, Kristof, Ren, Holm, Nair, Anita, Griffine, Brendan, Saal, Christoph, Kuentz, Martin, 2019. Application of the solubility parameter concept to assist with oral delivery of poorly water-soluble drugs – a PEARRL review. J. Pharm. Pharmacol. 71, 441–463.
Jiannan, Lu, Cuellar, Kristina, Hammer, Nathan I., Jo, Seongbong, Gryczke, Andreas, Kolter, Karl, Langley, Nigel, Repka, Michael A., 2016. Solid-state characterization of Felodipine-Soluplus® amorphous Solid Dispersions. Drug. Del. Ind. Pharm. 42 (3), 485–496.
Kamble, R.N., Bothiraja, C., Mehta, P.P., Varghese, V., 2017. Synthesis, solid state characterization and antifungal activity of ketoconazole cocrystals. J. Pharm. Investig. 48 (5), 541–549.
Karagianni, Anna, 2020. Production of itraconazole nanocrystal-based polymeric film formulations for immediate drug release. Pharmaceutics 12 (10), 960.
Keck, C.M., Mu, R.H., 2006. Drug nanocrystals of poorly soluble drugs produced by high pressure homogenisation. Eur. J. Pharm. Biopharm. 62 (1), 3–16.
Kitak, T., Dumicic, A., Planinšek, O., Šibanc, R., Srcic, S., 2015. Determination of solubility parameters of ibuprofen and ibuprofen lysinate. Molecules 20, 21549–21568.
Lee, J., Choi, J.Y., Park, C.H., 2008. Characteristics of polymers enabling nano-comminution of water-insoluble drugs. Int. J. Pharm. 355 (1–2), 328–336.
Li, J., Chiappetta, D., 2008. An investigation of the thermodynamic miscibility between VeTPGS and polymers. Int. J. Pharm. 350 (1–2), 212–219.
Liu, P., Viitala, T., Kartal-Hodzic, A., et al., 2015. Interaction studies between indomethacin nanocrystals and PEO/PPO copolymer stabilizers. Pharm. Res. 32 (2), 628–639.
Loh, Z.H., Samanta, A.K., Sia Heng, P.W., 2014. Overview of milling techniques for improving the solubility of poorly water-soluble drugs. Asian J. Pharm. Sci. 10 (4), 255–274.
Lu, Y., Wang, Z.H., Li, T., McNally, H., Park, K., Sturek, M., 2014. Development and evaluation of transferrin-stabilized paclitaxel nanocrystal formulation. J. Control. Release 176 (1), 76–85.
Malamatari, M., Ross, S.A., Douroumis, D., Velaga, S.P., 2017. Experimental cocrystal screening and solution-based scale-up cocrystallization methods. Adv. Drug Deliv. Rev.
Malamatari, M., Taylor, K.M.G., Malamataris, S., Douroumis, D., Kachrimanis, K., 2018. Pharmaceutical nanocrystals: production by wet milling and applications. Drug Discov. Today 23 (3), 534–547.
Martin, F., Pop, M., Borodi, G., Filip, X., Kacso, I., 2013. Ketoconazole salt and co-crystals with enhanced aqueous solubility. Cryst. Growth Des. 13 (10), 4295–4304.
McClements, D.J., 2011. Edible nanoemulsions: Fabrication, properties, and functional performance. Soft Matter 7 (6), 2297–2316.

Mithu, M.D.S.H., Economidou, S., Trivedi, V., Bhatt, S., Douroumis, D., 2021. Advanced methodologies for pharmaceutical salt synthesis. Cryst. Growth Des. 21 (2), 1358–1374.
Mittapelly, N., Rachumallu, R., Pandey, G., et al., 2016. Investigation of salt formation between memantine and pamoic acid: its exploitation in nanocrystalline form as long acting injection. Eur. J. Pharm. Biopharm. 101, 62–71.
Müller, R., Junghanns, 2008. Nanocrystal technology, drug delivery and clinical applications. Int. J. Nanomed. 3 (3), 295–309.
Muthuselvi, C., Arunkumar, A., Rajaperumal, G., 2016. Growth and characterization of oxalic acid doped with tryptophan crystal for antimicrobial activity. Der Chem Sin. 7 (4), 55–62.
Patel, M.R., Patel, R.B., Parikh, J.R., Solanki, A.B., Patel, B.G., 2011. Investigating effect of microemulsion components: in vitro permeation of ketoconazole. Pharm. Dev. Technol. 16 (3), 250–258.
Peltonen, L., 2018. Practical guidelines for the characterization and quality control of pure drug nanoparticles and nano-cocrystals in the pharmaceutical industry. Adv. Drug Deliv. Rev. 131, 101–115.
Peltonen, L., Tuomela, A., Hirvonen, J., 2015. Polymeric stabilizers for drug nanocrystals. Handb. Polym. Pharm. Technol. 4, 67–87.
SG Potta, S Minemi, RK Nukala, C Peinado, DA Lamprou, A Urquhart . Preparation and characterization of ibuprofen solid lipid nanoparticles with enhanced solubility. J. Microencapsul. 28 (1), 74-81.
WS Schlindwein, M Gibson. Pharmaceutical quality by design: a practical approach John Wiley & Sons.
Schwarz, C., Mehnert, W., 1999. Solid lipid nanoparticles (SLN) for controlled drug delivery II. drug in corporation and physicochemical characterization. J. Microencapsul. 16 (2), 205–213.
Serajuddin, A.T.M., 2007. Salt formation to improve drug solubility. Adv. Drug Deliv. Rev. 59 (7), 603–616.
Shayanfar, A., Jouyban, A., 2014. Physicochemical characterization of a new cocrystal of ketoconazole. Powder Technol. 262, 242–248.
Shegokar, R., Müller, R.H., 2010. Nanocrystals: Industrially feasible multifunctional formulation technology for poorly soluble actives. Int. J. Pharm. 399 (1–2), 129–139.
Shegokar, R., Singh, K.K., 2011. Surface modified nevirapine nanosuspensions for viral reservoir targeting: In vitro and in vivo evaluation. Int. J. Pharm. 421 (2), 341–352.
Tiago, J.M., Padrela, L., Rodrigues, M.A., Matos, H.A., Almeida, A.J., de Azevedo, E.G., 2013. Single-step co-crystallization and lipid dispersion by supercritical enhanced atomization. Cryst. Growth Des. 13, 4940–4947.
Toby, B.H., 2006. R factors in Rietveld analysis: how good is good enough? Powder Diffr. 21 (1), 67–70.
Tuomela, A., Hirvonen, J., Peltonen, L., 2016. Stabilizing agents for drug nanocrystals: effect on bioavailability. Pharmaceutics 8 (16), 1–18.
Vadher, B., Shah, S., Dudhat, K., Dhaval, M., Sing, S., Prajapati, B.G., 2024. Ketoconazole nanocrystals fortified gel for improved transdermal applications. Nanofabrication 9, 1885.
Van Eerdenbrugh, B., Van den Mooter, G., Augustijns, P., 2008. Top-down production of drug nanocrystals: Nanosuspension stabilization, miniaturization and transformation into solid products. Int. J. Pharm. 364 (1), 64–75.
Verwey, E.J., 1947. Theory of the stability of lyophobic colloids. J. Phys. Chem. 51 (3), 631–636.